Mass Spectrometry
DOI: 10.5702/massspectrometry.A0003

Review

In Situ Pressure Probe Sampling and UV-MALDI MS for Profiling Metabolites in Living Single Cells

Yousef Gholipour,[1] Rosa Erra-Balsells,[2] and Hiroshi Nonami*,[1]

[1] *Plant Biophysics/Biochemistry Research Laboratory, Faculty of Agriculture, Ehime University, Matsuyama, Japan*
[2] *CIHIDECAR-CONICET, Departamento de Quimica Organica, Facultad de Ciencias Exactas y Naturales, Universidad de Buenos Aires, Buenos Aires, Argentina*

In this work we describe the use of a combination of a cell pressure probe and a UV-matrix-assisted laser desorption/ionization time of flight (UV-MALDI-TOF) mass spectrometer for the *in situ* picoliter sampling and shotgun metabolite profiling of living single cells of plants. In addition to quantifiable sampling, the pressure probe has some unique features which differentiate it from other single-cell analytical tools. Cell wall and plasma membrane properties and water relations of *in situ* living single cells can be analyzed before sampling the cell sap. In addition, the fully-controlled sampling of cells located at different depths in plant tissues, measurement of the sample volume, and the addition of internal standards are facilitated by the pressure probe. Using a variety of organic compounds and nanoparticles as UV-MALDI matrices, metabolites from neutral carbohydrates to amino acids and other metabolites can be detected through UV-MALDI-TOF mass spectrometry analyses of picoliter-sized, single-cell samples.

Keywords: plant cell, metabolomics, single-cell metabolome, shotgun metabolite profiling, nanoparticles

(Received March 7, 2012; Accepted May 14, 2012)

INTRODUCTION

Life is most properly addressed and viewed as a complex system. The emerging field of systems biology seeks to examine this complexity based on a holistic approach. Holistic insights are provided by omics analyses of the composition of biosystems. On the other hand, the focus of modern biological research is moving from classical organ and tissue-level analyses to single cells, where the most fundamental events of life occur. Therefore, omics analyses with a single-cell resolution can explore the basic aspects of life, cell to cell variations, primary responses to abiotic stresses or various types of biotic attack, and the processes of growth or death. For such a molecular analysis of single cells, a reliable access to the cell sap, the ability to sampling in real time, and sensitive detection are critical. In this context, methodologies for single-cell omics analyses are being developed for the high-throughput exploration of biomolecules. Instrumentation and data processing for genomics and proteomics analyses of cells seem to be well-established.[1)] Metabolomics based on soft ionization mass spectrometry methods as the frontier of omics sciences, however, is emerging and it demands both methods and detection power.[2)] Different classical techniques such as NMR and mass spectrometry have been applied to metabolome analyses. Currently, for higher resolution, versatility, wide detection, structural elucidation and higher sensitivity, mass spectrometry is the top candidate.

Classically, biomolecules are extracted from biological tissues, separated, purified and finally analyzed by gas chromatography-mass spectrometry (GC-MS) or liquid chromatography-mass spectrometry (LC-MS). A modern high-throughput screening method, the shotgun analysis, has attracted considerable attention. Proteins, lipids or metabolites obtained from biological tissues or cells are infused directly into the ion source with minimal preparation beforehand.[3,4)] In the shotgun proteomic strategy, mixtures of proteins are digested into peptides and are then sequenced followed by an automated database searching.[5,6)] Both hardware and software for shotgun analyses of proteins have been developed.[6–8)] Corresponding to tissue analyses, single-cell metabolome analyses can follow one of above-mentioned strategies. *In vitro* cell solution analysis involves some single-cell omics analyses, which include cell lysis, homogenization, centrifugation and some purification steps. In this approach a number of cells are included for each analysis which provides analyte solutions in the sub-nanoliter range. The result is data that reflect average metabolite profiles, based on a few cells.[9–11)] The second approach, *in situ* single-cell analysis, is based on the direct, real time sampling of intact cells followed by metabolite profiling of the cell solution sample. In the case of plant cells, femtoliter to nanoliter sample volumes can be obtained. This shotgun approach can include the limited purification, as well. A number of reports describing successful *in situ* cell sampling and shotgun metabolite profiling are available (Table 1). In probe electrospray MS (PESI MS) *in situ* tissues are sampled by inserting a micrometer-order metal needle.[12)] The technique has been successfully applied to plant tissues.[13)] The needle can be inserted to a desired depth of the tissue to obtain deeper samples. The penetration of a nanoESI capillary tip, followed by direct electrospray of the cell solution with the aid of a solvent has been also reported[14,15)] and applied for the sampling of plant cells.[16)] The advantage of the latter technique is that the tip can be manipulated in the target cell under a microscope. In laser ablation electrospray ionization (LAESI)

* Correspondence to: Hiroshi Nonami, *Plant Biophysics/Biochemistry Research Laboratory, Faculty of Agriculture, Ehime University, Matsuyama, Japan*, e-mail: nonami@agr.ehime-u.ac.jp

Table 1. Examples of successful sampling and MS-based metabolite analyses of single cells.

Cell solution sampling method	Target cell	Sampling approach	Analysis resolution	Cell sample vol.	Sample volume measurement	Analyzed metabolites	Ion source and mass analyzer	Ref.
cell homogenates	yeast	*in vitro*	few-cell	nL	extract vol.	phosphorylated central metabolites	UV-MALDI TOF/TOF	9)
metal needle	plant cells	*in situ*	few-cell	fL–pL	—	amino acids, carbohydrates, secondary metabolites	PESI TOF	13)
– (direct gasification/ionization)	plant/animal cells	*in situ*	single-cell	pL (plant cells)	—	amino acids, carbohydrates	IR LESI Q-TOF	17)
cell homogenates	oocyte cells	*in vitro*	few-cell	nL	extract vol.	carbohydrates, organic acids, fatty acids	GC TOF	11)
micro-suction pipette	bone marrow	*in situ*	single-cell	—	—	histamine	UV-MALDI TOF	50), 51)
nanoESI capillary tip	animal cells	*in situ*	single-cell	—	—	histamine, leukotriene, serotonin	nanoESI Q-TOF	14)
nanoESI capillary tip	fibroblast cells	*in situ*	single-cell	fL	—	proline and unidentified small-molecule metabolites	nanoESI Q-TOF	15)
nanoESI capillary tip	plant cells	*in situ*	single-cell	pL	—	terpene alcohols	nanoESI LTQ-Orbitrap	16)
pressure probe capillary tip	plant cells	*in situ*	single-cell	pL	cell sample vol.	underivatized carbohydrates, amino acids, tuliposide A	UV-MALDI TOF	18)
capillary tip	plant gland cells	*in situ*	single-cell	—	—	flavonoids, naphthodianthrones and phloroglucinols	UV-LDI TOF	47)
cell homogenates	*E. coli*	*in vitro*	few-cell	—	—	phosphorylated central metabolites	UV-MALDI TOF	52)
quartz capillary tip	plant cells	*in situ*	single-cell	pL	cell sample vol.	anthocyanins	nanoLC-ESI IT	19)
glass capillary tip	plant cells	*in situ*	few-cell	—	extract vol.	sugars, amino acids, fatty acids, organic acids, alcohols, *etc.*	GC TOF	10)
quartz capillary tip	plant cells	*in situ*	single-cell	pL	cell sample vol.	phytoalexins	LC-ESI	20)

Table 2. Properties of *in situ* single cells measured with a cell pressure probe.

Properties	Equation		Explanation	Ref.
turgor	Ψ_P		direct measurement (see Fig. 5)	21)–24)
osmotic potential	Ψ_S		measuring freezing point of cell solution by a picoliter cryo-osmometer	23), 30), 31)
water potential	$\Psi_W = \Psi_P + \Psi_S$	(3)	Ψ_P: turgor and Ψ_S, osmotic potential	23), 31)
cell wall elastic modulus	$\varepsilon = \Delta\Psi_P/(\Delta V/V)$	(4)	$\Delta\Psi_P$: a change in pressure inside the capillary by a quick back and forth movement of a rod; ΔV: the change in the volume of the solution inside capillary during the manipulation; V: the volume of the corresponding cell (see Fig. 5)	22)–25)
cell wall extensibility	$m = G/(\Psi_P - Y)$	(5)	G: the relative growth rate at the elongation zone; Y: the yield threshold turgor; $(\Psi_P - Y)$: the growth-effective turgor	21)–23), 26)
hydraulic conductivity of plasma membrane	$L_P = (\ln 2 \times V)/(t_{1/2} \times A \times (\varepsilon - \Psi_S))$	(6)	V and A volume and surface of the cell; Ψ_S: osmotic potential; $t_{1/2}$: the half time needed for the pressure to return to its previous level after a step increase (see Fig. 5)	21)–25), 27)
cell volume	$V_o = \pi_o v/(P_o - P_e)$	(7)	π_o: osmotic pressure of the cell measured by a pico-cryo-osmometer; v: the aliquot volume in the capillary of the pressure probe; P_o and P_e original and final turgor values (see Fig. 5)	29)

mid-IR laser pulses are delivered through the tip of a glass fiber after inserting the tip into the superficial cells of tissues deposited on a surface.[17] Since the operation is monitored by a camera, it is possible to select a target cell and to localize the tip accurately. In LAESI MS, no measurement of the volume of the cell sample is possible.

For the quantitation of metabolites, femtoliter-picoliter volume of cell samples must be carefully handled and measured. Otherwise, the interpretation of the signal abundance as the relative natural change of metabolite content in cells cannot be reliable. With the above-mentioned methods, although the volume of samples is not accurately measured, it is possible to detect important metabolites and determine the relative abundance of the examined metabolites. Measurement of the sample volume is necessary for the accurate quantitation of metabolites. Additionally, accessing and sampling deeper cells with a capillary or a needle may not be straightforward. A few reports, including the present paper, demonstrate cell sample volume measurement.[18–20] We used a cell pressure probe for single-cell sampling followed by metabolite profiling with ultraviolet matrix-assisted laser desorption/ionization time-of-flight (UV-MALDI-TOF) MS.[18] The pressure probe facilitates both the sample volume measurement and deep cell sampling. In addition to cell sampling, several cell properties can be measured by the pressure probe (Table 2).

In this report, we review the achievements in the field of single cell MS metabolite analyses and explain the setup and operation of the pressure probe and its combined application with UV-MALDI MS for probing, measurable sampling, and shotgun metabolite profiling of *in situ* living single cells. Figure 1 displays the general set up for the pressure probe combined with UV-MALDI MS. Main steps in this technique include capillary tip localization; a target cell to transducer connection test; cell pressure probing and some other measurements; cell solution sampling with volume measurement; and finally, transferring the picoliter sample onto a MALDI plate followed by MS analyses. If necessary, adding a calibration solution (internal reference) to the cell sap sample with a controlled volume can be also achieved with the pressure probe.

CELL PRESSURE PROBE

Setup

Figure 2 shows a schematic illustration of a cell pressure probe. The pressure probe consists of a micro-capillary connected to a pressure transducer (*e.g.*, XTM-190 M-100G, Kulite Semiconductor Products Inc. in our lab), a piezo motor (*e.g.*, PM101 Märzhäuser Wetzlar, Germany in our lab) mounted on a 3D micro-manipulator, a motorized micrometer having a rotational metal rod, and its speed controller. The micro-capillary and the pressure transducer are connected with a silicon oil filled PEEK (polyether ether ketone) tube and a T-shaped metal connector. One side of the T-shaped connector is fit through a rubber seal together with the metal rod connected to the micrometer. The diameter of the rod is 0.3 mm. By rotating the micrometer with a speed-adjustable motor (*e.g.*, from Oriental Motor Co., Ltd., Japan in our lab), changes in the silicon oil volume in the pressure probe can be adjusted. To minimize vibration, the pressure probe and its accompanying instruments are

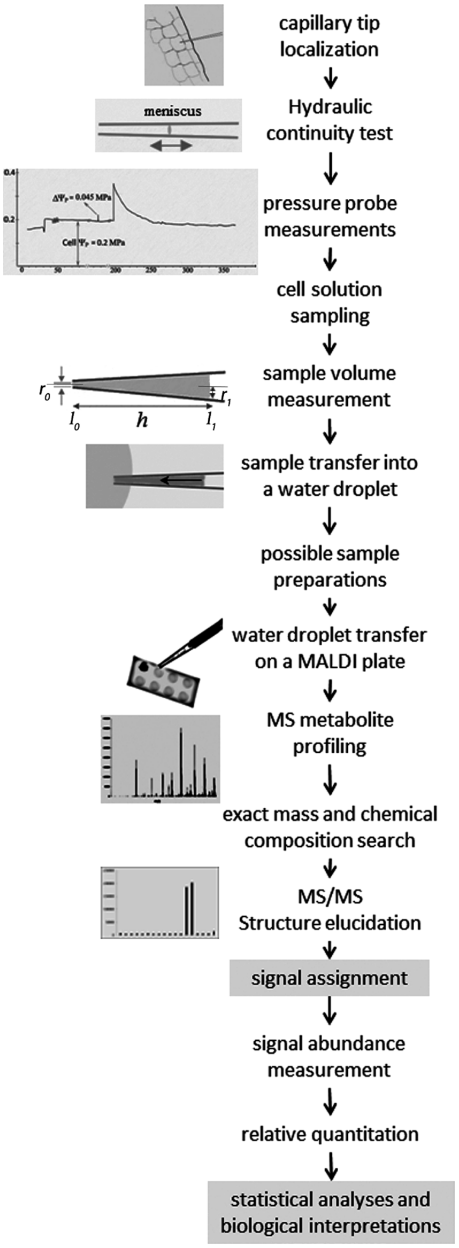

Fig. 1. The workflow of *in situ* single-cell metabolite analyses by the pressure probe and UV-MALDI MS combination.

placed on a magnetically-floated table. The manipulation of the capillary tip can be done with a high degree of accuracy. The operation is monitored under a digital microscope (*e.g.*, Keyence VHX-900 digital microscope in our lab) which facilitates recording the experiment and an online measurement of the sample volume. The pressure transducer is connected to a digital pressure display and a chart recorder. The pressure probing process is, therefore, monitored and recorded for further data analysis. The anatomy of the plant model has been previously studied and hence, the location and the depth of the target cells are known (Fig. 3). With a 3D manipulator, the capillary tip is located and penetrated by pushing the tip into the tissue by means of a piezo-motor. The depth of penetration can be monitored since a distance in the horizontal movement of the probe tip is displayed in the controller of the piezo-motor.

Since the composition and the thickness of plant cuticle and cell wall vary in plants, glass or quartz capillaries with different internal diameters and tip morphologies are used. Tapered capillaries with a preferred tip morphology can be prepared by adjusting the temperature, the pulling velocity and speed in a laser-heated micropipette capillary puller (*e.g.*, P-2000 Sutter Instrument in our lab). For plants with a thick cuticle, a short quartz capillary tip with an opening of 2–5 μm is required.

In normal plant cells, a hydraulic pressure is formed by turgor pressure which leads to an elastic expansion of the cell wall and with the cell volume maintained.[21–23] After penetration of the tip into a cell, the cell solution enters into the capillary tip due to the turgor pressure of the cell.[23,24] Since the cell solution is not soluble in silicon oil, two phases with a meniscus at the interface appear (Fig. 4A). When the tip enters the cell, the difference between cell turgor pressure and the oil pressure must not be too high, otherwise the cell may die due to membrane collapse after the cell solution comes out violently from the cell. A 0.5–1 bar difference can usually ensure a safe penetration, because non-stressed plant cells usually have 4–8 bars of turgor pressure in the cell.[23]

Both water and oil are incompressible, and since the whole system from the pressure transducer to the capillary tip is assembled so as to be air-tight, a sub-millibar change inside capillary tip is immediately sensed by the pressure transducer far from the capillary. On the other hand, pushing the rod inside the tubing using a micrometer connected to the speed-control motor correspondingly leads to a forward movement of silicon oil and a backward movement of cell solution. Since the diameter of the rod is 0.3 mm and the movement is in the nanometer-order, a sub-picoliter volume of oil or sample solution is conveniently handled. With each click on the speed adjustment buttons on the micrometer motor controller at the minimum speed, the rod is moved about 100 nm forward or backward. In practice, with the 0.3 mm radius of the rod and varying the viscosity and the surface tension of aqueous standard or cell solutions, 1–10 pL volume inside the tip can be handled. With some practice (and possibly with a long tip and smaller opening), an experimenter can remove a femtoliter solution, as well. To do so, while sucking a standard or cell solution into the capillary tip, the capillary is rapidly pulled out of the droplet, resulting in the capture of a femtoliter volume of the solution inside the tip. However in this case, unlike the case of picoliter sampling, collecting a pre-determined or a specific volume of analyte solution may not be straightforward.

Measurements

Before any measurements, a hydraulic continuity test[25] is performed (Fig. 5). Pressure is decreased and increased quickly several times and if the meniscus can be moved back and forth correspondingly, it will show a perfect hydraulic connection between the target cell and the pressure transducer.[25] Additionally, while the tip has been already inserted into the inside of a cell, the pressure is kept unchanged for a period and if the pressure and the meniscus location remain unchanged, it confirms that no cell solution has leaked. Afterward, single-cell pressure probe measurements can be reliably carried out (Fig. 5). Managing the location of the meniscus and measuring oil pressure inside capillary are core operations in pressure probe technique. For example, the pressure needed to return the meniscus to its original

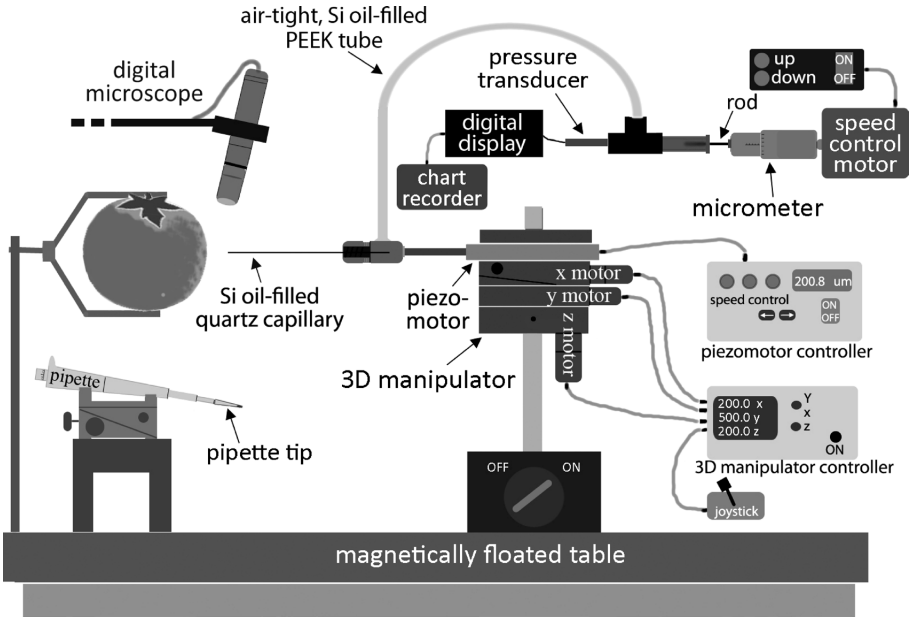

Fig. 2. A schematic illustration of a cell pressure probe. The localization and the penetration of the capillary tip into the plant tissue are fully controlled. Since the tubing is air-tight, the instrumentation can be used for pressure probing and *in situ* sampling of living single cells. The picoliter cell solution sample is then transferred to a water droplet at the tip of a pipette to facilitate its final transfer onto a UV-MALDI plate. The entire operation is monitored and photographed by a digital microscope.

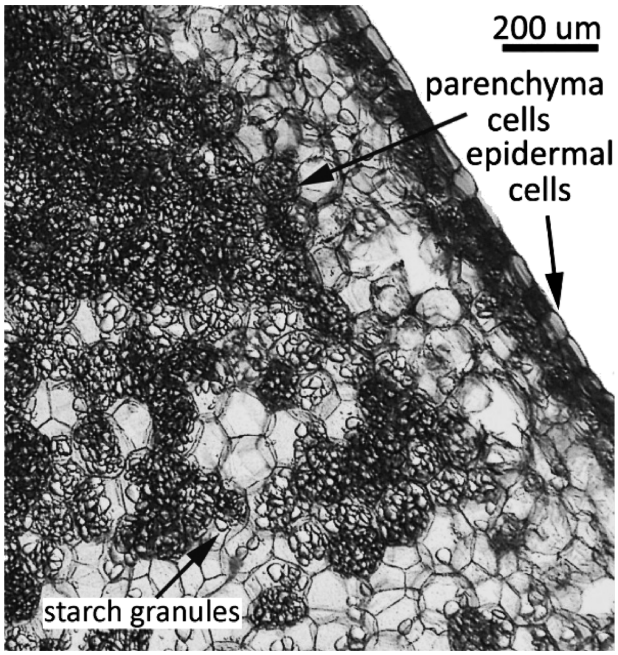

Fig. 3. Photo of a cross-section of the second scale of a tulip bulb; parenchyma cells with abundant starch and soluble oligosaccharides are shown. Mass spectra in Fig. 10 and data in Fig. 11 provide molecular information about these cells.

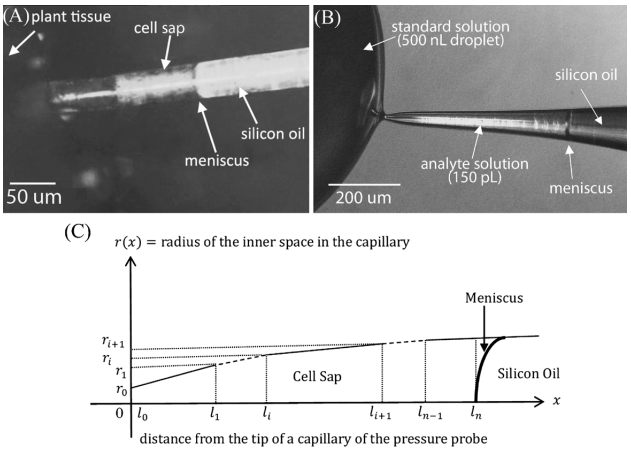

Fig. 4. (A) Photo of a pressure probe capillary which was inserted into a cell, having the meniscus between cell sap and the silicon oil. (B) Photo of the meniscus formed between the analyte solution and silicon oil inside the capillary. (C) Schematic illustration of changes in the radius, $r(x)$, of the inner space in the capillary from the tip (*i.e.*, l_0) to the location of meniscus (*i.e.*, l_n) formed between cell sap and the silicon oil. See Eqs. (1) and (2) which use the symbols and their definitions.

position where it was before the tip had penetrated the cell, is equal to the turgor of that cell (Fig. 5). In addition to the cell turgor, several other properties of a cell can be measured with the pressure probe (Table 2). By meniscus management, cell wall elastic modulus,[23, 25] cell wall extensibility,[26] hydraulic conductivity[24–28] of the plasma membrane, and the volume of the target cell[29] can also be measured (Fig. 5). A part of the cell solution sample inside the capillary tip can be transferred to a picoliter cryo-osmometer plate[23,30,31] (Fig. 6). Subsequently, the osmotic potential of the cell is directly measured with a picoliter cryo-osmometer (*e.g.* Clifton Technical Physics, USA in our lab).[23] Water potential, a central concept in cell biology, is then uniquely calculated with a single-cell resolution (water potential equals turgor plus osmotic potential).[23,31] Analyzing these properties significantly contribute to our understanding of growth or stress responses and adaptations at the cellular level.[23]

PICOLITER CELL SAMPLING

After pressure probe measurements, the cell sap is

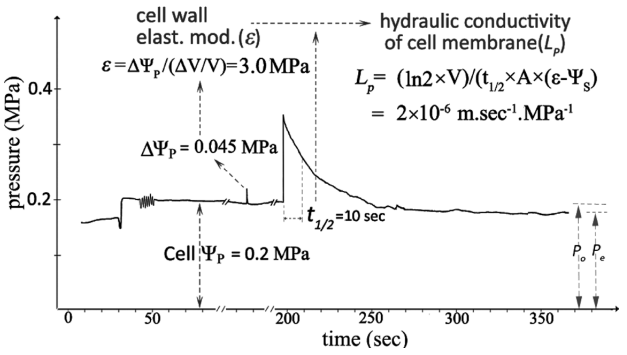

Fig. 5. Monitoring hydraulic pressure inside the capillary tip of a cell pressure probe which allows *in situ* measurement of several cell properties defined in Table 2. P_o and P_e values are used in cell volume measurements.

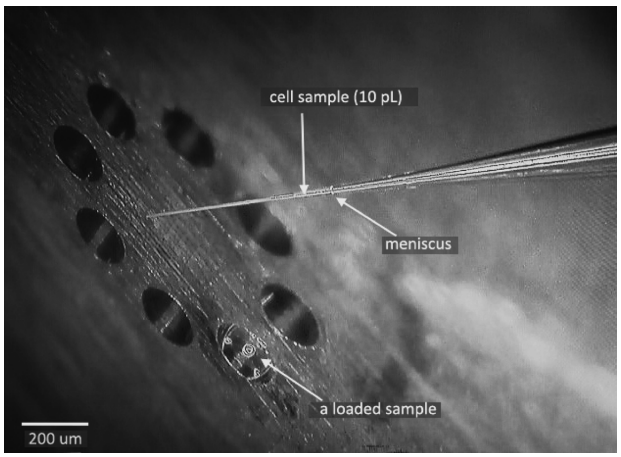

Fig. 6. Photo showing that a part of a cell sap sample can be transferred to a picoliter cryo-osmometer plate for osmotic potential measurements.

sampled. After taking the sample from a target cell located at a known depth, the capillary tip is taken out of the tissue while the oil pressure is controlled, in order to preserve the sample inside the tip. The dimensions of the cell sample can be immediately measured under the microscope, the volume of the truncated cone-shaped sample is calculated, and the tip with the sample inside is photographed to record the experiment.

The volume of the cell sap inside the capillary tip (Fig. 4A) can be determined by measuring the radius ($r(x)$) with respect to a distance from the tip (l_0) up to the location of the meniscus (l_n) as illustrated in Fig. 4C. By balancing the pressure inside the capillary against the atmospheric pressure, the surface tension at the tip can hold the cell sap in the capillary. The radius of the inner wall of the capillary ($r(x)$) can be expressed as a linear function of the distance (x) from the tip, and piecewise linear lines can be extended from the tip to the location of the meniscus between cell sap and silicon oil (as shown in Fig. 4C) *i.e.*

$$r(x)=\left(\frac{r_{i+1}-r_i}{l_{i+1}-l_i}\right)(x-l_i)+r_i \quad (1)$$

($r(x)$: *a linear function in* $l_i \le x \le l_{i+1}$;

$r(x)=r_0$ *at* $l_0=0$; $i=0, 1,..., n$)

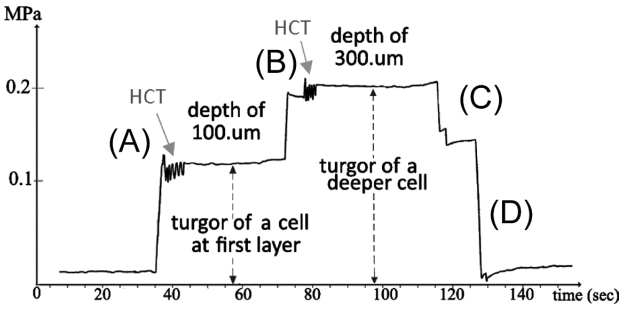

Fig. 7. Deep cell turgor probing and sampling with a pressure probe. (A) with an oil pressure of 0.5–1 bar less than the cell turgor, the capillary tip is inserted into a shallower cell; a hydraulic continuity test (HCT) is performed to ensure the proper localization of the tip and perfect connection between the pressure transducer and the target cell; pressure is raised to measure the turgor of first cell; (B) the tip is inserted into the deeper cell; HCT is performed; and turgor is measured; (C) pressure is decreased to allow the deep cell solution to enter into the capillary tip; (D) while capillary tip is pulled out of the tissue pressure is quickly reduced to about atmospheric pressure to retain the cell sample inside the capillary tip.

The lines can be revolved around the x-axis, and the volume ($V(x)$) of cell sap in the capillary can be calculated as follows;

$$V(x)=\sum_{i=0}^{n-1}\pi\int_{l_i}^{l_{i+1}} r(x)^2\,\mathrm{d}x \quad (2)$$

($r(x)$: *a linear function in* $l_i \le x \le l_{i+1}$)

Deep cell sampling is another unique feature of the pressure probe. While moving the capillary tip through the cell layers and until it reaches a target cell, the cell solution can easily be prevented from entering the tip by regulating the oil pressure (Fig. 7). After sampling, a picoliter volume of compatible standard chemicals with a known concentration can be added to the cell solution sample inside the capillary tip, as shown in Fig. 4B. These compounds can be used for internal calibration and for a comparison of the relative abundance of cell metabolites. At the end of the pressure probe operation, a cell sample with a known volume, pressure probe measurement data, a paper record of the probing process, and digital photos (and videos) of the operation are available. Nonami and Boyer[28] discussed possible errors in detail during the pressure probe operation in cell sap sampling.

For transferring a cell sample onto the UV-MALDI plate, the tip is located inside a water droplet and the sample is injected by inserting a small pressure. The volume of a water droplet in an Eppendorf pipette tip can be measured accurately by weighing the droplet and the pipette on an electric ultra-microbalance with accuracy of 0.1 μg, *i.e.*, equivalent of 0.1 nL. The volume of the water droplet may influence the quality of sample on the plate; the localization of the sample after drying may change with a small or large droplet deposited on a dried layer of matrix. The change in the volume of a water droplet inside the pipette tip is negligible for about 10 min at room temperature (Fig. 8). On the other hand, the whole process of transferring the sample into the water droplet and depositing a droplet of the mixture of the sample and the water droplet on a previously air-dried

matrix layer on the plate usually requires 1–3 min. For convenience, we use 0.5 μL droplets for transferring cell samples (Fig. 4B). Before UV-MALDI MS analyses, if necessary, a sample preparation step can be also added to the workflow (see below).

MS ANALYSES

UV-MALDI MS

Finding a proper matrix for a specific group of chemicals is a big challenge in UV-MALDI MS, as there are no clear criteria for the selection of the matrix, which is largely empirical.[32,33] In the case of shotgun metabolite profiling, a wide range of compounds from carbohydrates, amino acids, organic acids, secondary metabolites and fatty acids can be examined. Even after sample purification and separation, diverse types of metabolites may still be present in the mixture. Furthermore, in mass spectrometry-based, single-cell metabolomics, the limit of detection and the need for the relative quantitation make the matrix challenge bigger. Among organic matrices for the UV-MALDI MS metabolite profiling of plant cell samples, 2,4,6-trihydroxyacetophenone (THAP), 2,5-dihydroxybenzoic acid (DHB), and 9-aminoacridine are commonly used (Table 3). In the case of THAP, with a nearly uniform deposition on the plate, the likelihood of the co-existence of sample and matrix molecules in a location on the plate is quite high, compared to DHB, which has a tendency to crystallize (Fig. 9). Additionally, a more diverse range of metabolites can be detected with THAP. Another common matrix in UV-MALDI MS analyses, 3,5-dimethoxy-4-hydroxycinnamic acid (sinapinic

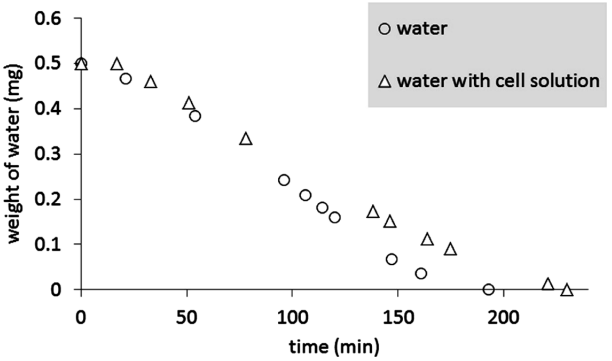

Fig. 8. Changes in the weight of water (○) and that of water with cell sap (△) measured using an electric ultra-microbalance while 0.5 μL of the droplet was kept in an Eppendorf pipette tip at room temperature. For about 10 min the weight loss due to evaporation is negligible. Therefore, transferring the cell solution sample to a water droplet and then onto the UV-MALDI plate, which is usually carried out within 1–3 min, is reliable.

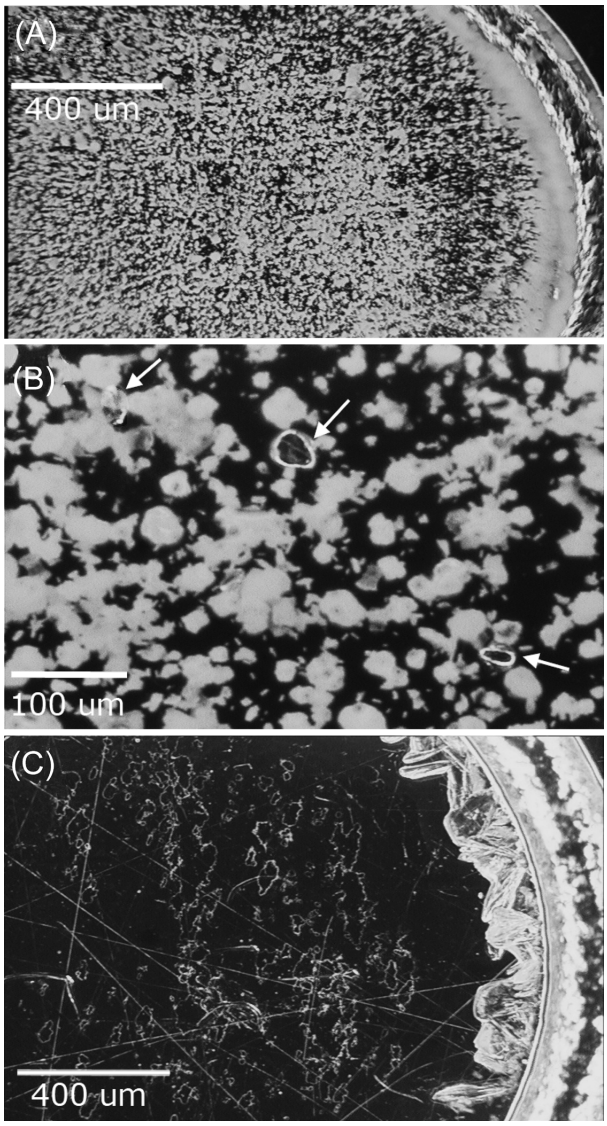

Fig. 9. Photos of THAP (A), cell samples with THAP (B) and DHB (C) after air-drying on a gold UV-MALDI plate. Arrows in (B) point the locations of small aggregates of a dried pico-liter cell sample deposited on THAP. While after drying THAP covers a spot almost uniformly, big DHB crystals located mainly at the edge.

Table 3. List of compounds examined as IR- and UV-MALDI MS matrices for metabolite analyses of plant cells.

Matrix	Ion mode of analysis	Laser, λ (nm)	Analyzed metabolites	Ref.
DHB	(+)	N_2 UV, 337	histamine	50)
DHB	(+)	N_2 UV, 337	histamine	51)
CHCA*, DHB	(+)		histamine	45)
THAP, DHB, CNTs	(+)	N_2 UV, 337	carbohydrates	18)
9-aminoacridine	(−)	N_2 UV, 337	phosphorylated, ATP, ADP, GDP, *etc.*	46)
9-aminoacridine	(−)	N_2 UV, 337; Nd: YAG, UV, 355	chosphorylated metabolites	52)
native water; DHB, succinic acid, thiourea, glycerol	(−)	Nd: YAG, IR, 2940	organic acid, carbohydrates, *etc.*	17), 49)

*α-Cyano-4-hydroxycinnamic acid.

Table 4. The efficiency of MALDI matrices examined by our group for direct UV-MALDI MS metabolite profiling of *in situ* plant tissues and single cells.

Matrix		Ion mode	Detection suitability	LOD*	Linearity signal abundance *vs.* conc.	Ref.
organic	THAP	(+) and (−)	carbohydrates, amino acids, organic acids, secondary metabolites	(+) low(−) aver.	average	18), 42), 44)
	DHB	(+) and (−)	carbohydrates, amino acids	(+) low(−) aver.	low	18), 42), 44)
	norHo	(−)	organic acids, secondary metabolites	(−) high	—	18), 42), 44)
nanoparticles	diamond	(+)	carbohydrates	(+) high	—	42)
	$(SiO_2)(TiO_2)$	(+) and (−)	carbohydrates, organic acids, secondary metabolites	(+) low	very high	42), 44)
	$(BaTiO_3)(SrTiO_3)$	(+) and (−)	carbohydrates	(+) low	high	42)
	TiO_2	(+) and (−)	carbohydrates	(+) low	very high	42)
nanotubes	CNTs	(+)	carbohydrates	(+) high	low	18), 42), 43)

*Limit of detection (LOD).

acid), can be evaluated for its potential efficiency in single-cell metabolite analyses by UV-MALDI MS.

We have examined[18] some common organic matrices already introduced by other authors for the UV-MALDI MS of biomolecules including THAP[34] and DHB[35] as well as 9*H*-pyrido[3,4-*b*]indole (norHo) and extensively studied its properties and applications,[36–41] for their usefulness in plant single-cell metabolite profiling. Additionally, we have introduced a number of new matrices for the UV-MALDI MS metabolite profiling of plants including the nanoparticles (NPs) of titanium silicon oxide ($(SiO_2)(TiO_2)$), barium strontium titanium oxide ($(BaTiO_3)(SrTiO_3)$), titanium oxide (TiO_2),[42] and carbon nanotubes (CNTs).[43] Table 4 summarizes our current knowledge regarding the efficiency of matrices used in plant metabolite analyses. Sugars, including simple saccharides and fructans, play important roles in plant cell growth and stress tolerance. Therefore, the availability of matrices to desorb/ionize these chemicals is quite helpful in the area of plant physiology. Nanoparticles are powerful matrices for UV-MALDI MS analyses of underivatized carbohydrates. The low limit of detection (LOD) and high linearity response of NPs make them a matrix of choice for detecting (Fig. 10) and quantifying underivatized carbohydrates by UV-MALDI MS (Fig. 11).

In our UV-MALDI MS analyses of single-cell samples, for each sample spot on the plate, 15 tiles each $400\times400\,\mu m^2$, 10 at the edge and 5 at the center are determined. Each tile is shot with 400 laser pulses and is separately saved. Regarding the dimension and the distribution of dried cell sample on the plate and the size of the tile, it appears that 1–2 tile(s) can be sufficient localize all cell sample aggregates (Fig. 9). The resulting mass spectra with cell metabolite signals are used for further analyses and reporting. Since the number of cell metabolite molecules is in the range of attomoles to picomoles, therefore, after 400 laser shots, almost all of the cell metabolites located in the irradiation area are desorbed and ionized.

Although still developing, some extensive plant metabolite databases are available for comparing the exact mass

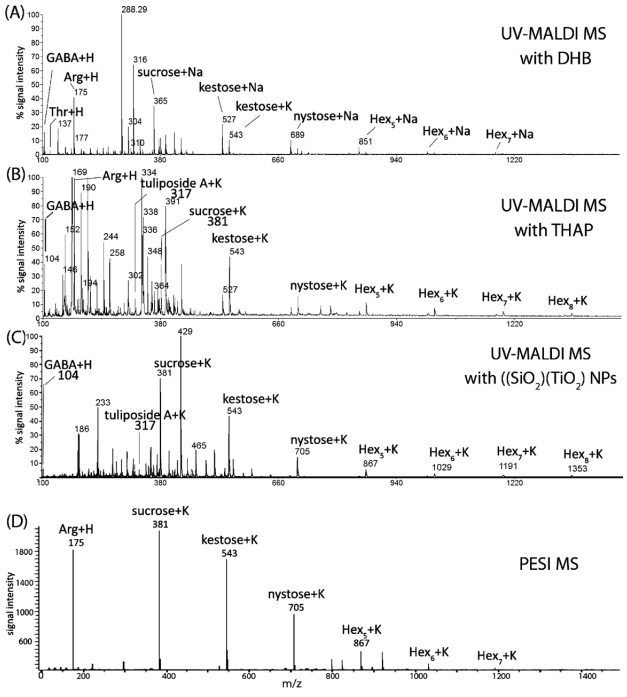

Fig. 10. (A–C) UV-MALDI TOF MS mass spectra of tulip bulb cell sap sampled directly with the pressure probe are compared with (D) an ESI-based MS (PESI MS) mass spectrum acquired by analyzing *in situ* tulip bulb tissues. (A), (B), and (C) unpublished data from ref. 44; and (D) adopted with permission from ref. 13. ©2009 Elsevier.

values of putative metabolite signals. A network of plant metabolic databases (http://www.plantcyc.org/) has been established that contributes the plant metabolome analyses by providing information regarding genes, enzymes, pathways and compounds. Signal assignments in our UV-MALDI MS analyses are based on several approaches including exact mass value searches, the elemental composition analysis, physiology information and the literature review. Since the number of molecules of metabolites in a picoliter cell

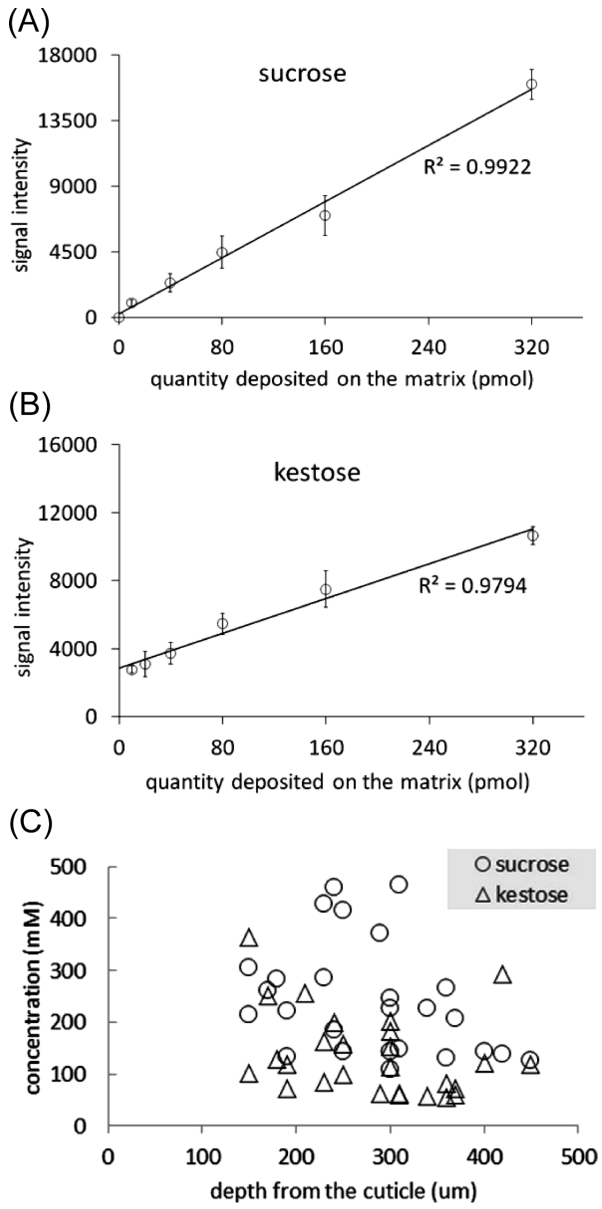

Fig. 11. Plots between the signal intensity and the number of moles of standard sucrose (A) and kestose (B) deposited as an aqueous solution on $(SiO_2)(TiO_2)$ NPs, and (C) cell sap analyses with respect to the depth from the cuticle surface of a tulip bulb (see Fig. 3). About 150–800 pL samples could be obtained from each cell. Sucrose and kestose were abundant in those cells and yielded peaks with substantial intensities in the positive ion mode (see Fig. 10). (A) and (B) adapted with permission from ref. 42 ©2010 American Chemical Society; (C) unpublished data, ref. 44.

sample are not high, resulting in a low signal abundance, a small part of the plant tissue where single-cell analyses are performed is sampled, homogenized and the soluble compounds are extracted for the MS/MS analysis of detected metabolites.

Several metabolites from sugars, amino acids, secondary metabolites and organic acids can be detected with the matrices introduced here. Underivatized sugars, hexoses (fructose and glucose), Hex_2 (mostly sucrose) and oligosaccharides from Hex_3 (kestose) to Hex_{15} have been detected in picoliter single-cell samples. It is possible to detect ascorbic acid, a secondary product of sugar metabolism, as well. Among the amino acids, proteinogenic amino acids (*e.g.* Pro, Gln, Arg, Thr, and Glu) and choline; and from organic acids, citric acid and malic acid could be detected in cell samples. We have also identified polyamine putrescine and tuliposide A.[44] Figure 10 shows the acquisition of metabolite signals by two MALDI-based and ESI-based tools. These methods had been applied to the analysis of cell solutions obtained from tulip bulbs and, interestingly, the results were very similar. Using the combination of a pressure probe and UV-MALDI MS, however, more metabolites could be detected and additionally, as mentioned above, the sample volume could be measured accurately. Analyzing MS metabolite profiles has not been automated and is time-consuming which makes it a significant challenge in single-cell analyses.

Another challenge in shotgun metabolite profiling by UV-MALDI MS is signal suppression. This can originate from abundant salts that are naturally present in cell solutions, interfering metabolites such as lipids, and from the competition between biomolecules during the ionization. Sample purification can improve the acquisition of metabolite signals from a cell mixture solution. The amounts of interfering metabolites in a cell sample and the extent of the signal suppression determines whether or not to include a purification step. For example, in some plants, parenchyma cells contain huge amounts of stored oils or lipids which adversely affect the signal yield of sugars and small metabolites. For extracting lipids from cell solution samples, 1 μL of chloroform can be added to a 1 μL water droplet containing a cell solution inside a microcentrifuge tube. Commercial microliter filters, *i.e.* Millipore ZipTip® pipette tips with chromatography media fixed at their tips, can be used for further single-cell sample preparations including concentrating, separating or desalting biomolecules. Single-cell solution preparations may result in the loss of the signal of less abundant metabolites and can reduce the signaling yield of underivatized sugars which usually ionize as potassiated and sodiated cations in the positive ion mode. Therefore, protocols for preparations need to be carefully assessed and are most useful for targeted metabolite profiling.

Although the UV-MALDI technique is not necessarily a quantitative tool, signal abundance can be used, to some extent, to explore relative changes in the natural abundance of metabolites. THAP and metal nanoparticles have shown the capability to desorb/ionize carbohydrates in cell or tissue samples.[18,45,46] The linearity between signal abundance and the number of molecules of sugar standards deposited on $(SiO_2)(TiO_2)$ NPs is shown in Figs. 11A, B. This is the matrix of choice for the UV-MALDI MS analyses of small sugars and oligosaccharides. High linearity of standards acquired with this matrix helped to examine relative concentration of sucrose and kestose in cell samples (Fig. 11C). In order to improving the accuracy of the relative quantitation by the UV-MALDI MS of cell samples, internal standards with known picoliter volumes and concentrations can be also added to cell samples inside the pressure probe capillary tip.

Laser Desorption/Ionization MS and IR-MALDI MS

The majority of cell metabolites require a matrix to use the energy of UV laser photons for desorbing/ionizing. However, some metabolites with benzene rings or those that contain a rich conjugated system in their molecular

structure, *e.g.* flavonoids, naphthodianthrones and phloroglucinols, can absorb UV at 337 nm and therefore, can be studied by matrix-free laser desorption/ionization (LDI) MS.[47)]

It has been shown that native water, DHB, succinic acid, thiourea and glycerol could serve as IR-MALDI MS matrices for the direct desorption/ionization of a wide range of metabolites from a number of cells that are located on the surface of plant tissues.[48,49)] The technique was later applied to directly ablate metabolites from intact plant single cells with native water as the matrix.[17)]

MALDI-MS *vs.* ESI-MS

In contemporary mass spectrometry, two powerful soft ionization techniques MALDI and ESI MS are employed for metabolite profiling. Based on our experience, we compare the applicability of these distinct ion sources in single-cell shotgun metabolomics. The first noticeable difference can be attributed to salt tolerance. In shotgun analyses, samples of cell sap can naturally contain a high levels of salts. In many plants, for instance, potassium is an abundant intracellular compound. The quality of ESI MS metabolite profiling of single-cell samples can be adversely influenced by the inherent susceptibility of ESI to high salt levels. Purification of the sample may improve the results but, as mentioned above, may raise another problem, namely, the loss of analyte molecules. We have frequently observed a higher relative signal abundance of many metabolites in MALDI mass spectra compared to their abundance in ESI mass spectra. In ESI MS, in addition, minor changes in solvent spraying, flow rate *etc.* may significantly change the quality of the results. In the plant sciences, underivatized neutral carbohydrates ranging from monohexoses to long-chained oligosaccharides play important roles in metabolism, growth and the response to environmental stresses. Overall, our experience indicates that single-cell MALDI MS is more efficient for the analysis of underivatized, plant-derived carbohydrates; in plant tissue and cell samples, oligosaccharides with a high degree of polymerization (*e.g.* with 15 moieties) could only be detected using MALDI MS. On the other hand, due to the specificity of MALDI matrices, metabolites detected in cell samples may be less diverse in MALDI MS. In our experiments related to the profiling of single-cell metabolites, we have frequently observed lower signal acquisition yields in the negative ion mode when examined matrices were employed, and therefore, we have concluded that nanoESI MS is the preferred technique for profiling negatively charged metabolites.

OPPORTUNITIES AND CHALLENGES

Single-cell metabolomics is the analysis of the phenotype with the highest resolution and has great potential for contributing to the enhancement of cell systems biology. The joint application of a pressure probe and a UV-MALDI system facilitates the acquisition of data related to physical properties and the molecular composition of *in situ* living single cells; which means that an experimenter can develop wider and deeper insights into the events during growth or stress responses with a single-cell resolution. However, there continues to be a need for further improvements in sensitivity of detection. Additionally, almost all software in the field has been developed for chromatography-mass spectrometry based data acquisition and processing. For shotgun UV-MALDI MS metabolomics, developing software that is capable of directly extracting information from mass spectra, that can automatically search libraries and databases and finally is able to analyze relative quantitative data carries a high priority. The shotgun approach is very beneficial to omics analyses, but the signal yield of metabolites in cell mixture samples needs to be improved. The purification of cell solution samples can improve the signal acquisition of targeted metabolites. However, sample loss should be minimized. Although identifying a universal matrix for the UV-MALDI-based metabolite profiling remains a difficult task, examining potential matrices for the laser desorption/ionization of larger numbers of metabolites and to decrease the limit of detection is clearly a worthwhile objective.

Acknowledgements

The authors are grateful for the financial support of a Grant-in-Aid (S) from the Japan Society for the Promotion of Science (JSPS) for Scientific Research (24228004), University of Buenos Aires, Argentina (X088) and CONICET, Argentina (PIP 00400). R.E.B. is research member of CONICET (Argentina).

REFERENCES

1) A. Amantonico, P. L. Urban, R. Zenobi. *Anal. Bioanal. Chem.* 398: 2493–2504, 2010.
2) A. Avatoš. *Anal. Chem.* 83: 5037, 2011.
3) X. Han, K. Yang, R. W. Gross. *Mass Spectrom. Rev.* 31: 134–178, 2012.
4) G. Sun, K. Yang, Z. Zhao, S. Guan, X. Han, R. W. Gross. *Anal. Chem.* 79: 6629–6640, 2007.
5) A. J. Link, J. Eng, D. M. Schieltz, E. Carmack, G. J. Mize, D. R. Morris, B. M. Garvik, J. R. Yates 3rd. *Nat. Biotechnol.* 17: 676–682, 1999.
6) A. I. Nesvizhskii, R. Aebersold. *Mol. Cell. Proteomics* 4: 1419–1440, 2005.
7) S. P. Gygi, B. Rist, S. A. Gerber, F. Turecek, M. H. Gelb, R. Aebersold. *Nat. Biotechnol.* 17: 994–999, 1999.
8) M. P. Washburn, D. Wolters, J. R. Yates 3rd. *Nat. Biotechnol.* 19: 242–247, 2001.
9) A. Amantonico, J. Y. Oh, J. Sobek, M. Heinemann, R. Zenobi. *Angew. Chem. Int. Ed.* 47: 5382–5385, 2008.
10) B. Ebert, D. Zöller, A. Erban, I. Fehrle, J. Hartmann, A. Niehl, J. Kopka, J. Fisahn. *J. Exp. Bot.* 61: 1321–1335, 2010.
11) M. M. Koek, F. Bakels, W. Engel, A. van den Maagdenberg, M. D. Ferrari, L. Coulier, T. Hankemeier. *Anal. Chem.* 82: 156–162, 2010.
12) K. Hiraoka, K. Nishidate, K. Mori, D. Asakawa, S. Suzuki. *Rapid Commun. Mass Spectrom.* 21: 3139–3144, 2007.
13) Z. Yu, L. C. Chen, H. Suzuki, O. Ariyada, R. Erra-Balsells, H. Nonami, K. Hiraoka. *J. Am. Soc. Mass Spectrom.* 20: 2304–2311, 2009.
14) H. Mizuno, N. Tsuyama, T. Harada, T. Masujima. *J. Mass Spectrom.* 43: 1692–1700, 2008.
15) N. Tsuyama, H. Mizuno, E. Tokunaga, T. Masujima. *Anal. Sci.* 24: 559–561, 2008.
16) M. L. Tejedor, H. Mizuno, N. Tsuyama, T. Harada, T. Masujima. *Anal. Sci.* 25: 1053, 2009.
17) B. Shrestha, A. Vertes. *Anal. Chem.* 81: 8265–8271, 2009.
18) Y. Gholipour, H. Nonami, R. Erra-Balsells. *J. Am. Soc. Mass Spectrom.* 19: 1841–1848, 2008.

19) S. Kajiyama, K. Harada, E. Fukusaki, A. Kobayashi. *J. Biosci. Bioeng.* 6: 575–578, 2006.
20) Y. Izumi, S. Kajiyama, R. Nakamura, A. Ishihara, A. Okazawa, E. Fukusaki, Y. Kanematsu, A. Kobayashi. *Planta* 229: 931–943, 2009.
21) P. J. Kramer, J. S. Boyer. *Water Relations of Plants and Soils*, Academic Press, San Diego, 1995.
22) J. S. Boyer. *Measuring the Water Status of Plants and Soils*, Academic Press, San Diego, 1995.
23) H. Nonami. *Plant Water Relations* (Japanese in text), Yokendo, Tokyo (2001).
24) D. Hüsken, E. Steudle, U. Zimmermann. *Plant Physiol.* 61: 158–163, 1978.
25) E. Steudle, U. Zimmermann, U. Luttge. *Plant Physiol.* 59: 285–289, 1977.
26) P. B. Green, R. O. Erickson, J. Buggy. *Plant Physiol.* 47: 423–430, 1971.
27) H. Nonami, J. S. Boyer. *Plant Physiol.* 93: 1610–1619, 1990.
28) H. Nonami, J. S. Boyer. *Plant Physiol.* 102: 13–19, 1993.
29) M. Malone, A. D. Tomos. *Planta* 182: 199, 1990.
30) K. A. Shackel. *Plant Physiol.* 83: 719–722, 1987.
31) H. Nonami, E. D. Schulze. *Planta* 171: 35–46, 1989.
32) E. de Hoffmann, V. Stroobant. *Mass Spectrometry: Principles and Applications,* 3rd Ed., Wiley-Interscience, London (2007).
33) R. B. Cole. *Electrospray and MALDI Mass Spectrometry: Fundamentals, Instrumentation, Practicalities, and Biological Applications*, 2nd Ed., John Wiley & Sons, Inc., London (2010).
34) J. Krause, M. Stoeckli, U. P. Schlunegger. *Rapid Commun. Mass Spectrom.* 10: 1927–1933, 1996.
35) U. Bahr, M. Karas, F. Hillenkam. *Fresenius J. Anal. Chem.* 348: 783–791, 1994.
36) H. Nonami, S. Fukui, R. Erra-Balsells. *J. Mass Spectrom.* 32: 287–296, 1997.
37) H. Nonami, K. Tanaka, Y. Fukuyama, R. Erra-Balsells. *Rapid Commun. Mass Spectrom.* 12: 285–296, 1998.
38) R. Erra-Balsells, H. Nonami. *ARKIVOC*. X: 517, 2003.
39) M. Mesaros, O. I. Tarzi, R. Erra-Balsells, G. M. Bilmes. *Chem. Phys. Lett.* 426: 334–340, 2006.
40) R. Erra-Balsells, H. Nonami. *Environ. Control in Biol.* 46: 65, 2008.
41) O. I. Tarzi, H. Nonami, R. Erra-Balsells. *J. Mass Spectrom.* 44: 260–277, 2009.
42) Y. Gholipour, S. L. Giudicessi, H. Nonami, R. Erra-Balsells. *Anal. Chem.* 82: 5518–5526, 2010.
43) Y. Gholipour, H. Nonami, R. Erra-Balsells. *Anal. Biochem.* 383: 159–167, 2008.
44) Y. Gholipour, H. Nonami, R. Erra-Balsells. unpublished data.
45) Y. Hirakawa, M. Shimizu, T. Masujima. *Bunseki Kagaku* 53: 519–526, 2004.
46) A. Amantonico, P. L. Urban, S. R. Fagerer, R. M. Balabin, R. Zenobi. *Anal. Chem.* 82: 7394–7400, 2010.
47) D. Hölscher, R. Shroff, K. Knop, M. Gottschaldt, A. Crecelius, B. Schneider, D. G. Heckel, U. S. Schubert, A. Svatoš. *Plant J.* 60: 907–918, 2009.
48) Y. Li, B. Shrestha, A. Vertes. *Anal. Chem.* 79: 523–532, 2007.
49) Y. Li, B. Shrestha, A. Vertes. *Anal. Chem.* 80: 407–420, 2008.
50) M. Shimizu, F. Levi-Schaffer, N. Ojima, T. Shingaki, T. Masujima. *Anal. Sci.* 18: 107–108, 2002.
51) M. Shimizu, N. Ojima, H. Ohnishi, T. Shingaki, Y. Hirakawa, T. Masujima. *Anal. Sci.* 19: 49–53, 2003.
52) D. Yukihira, D. Miura, K. Saito, K. Takahashi, H. Wariishi. *Anal. Chem.* 82: 4278–4282, 2010.

